

STSC-SNN: Spatio-Temporal Synaptic Connection with Temporal Convolution and Attention for Spiking Neural Networks

Chengting Yu^{1,2}, Zheming Gu¹, Da Li¹, Gaoang Wang², Aili Wang^{1,2,*}, Erping Li^{1,2}

¹ College of Information Science and Electronic Engineering, Zhejiang University, Hangzhou, China

² ZJU-UIUC Institute, Zhejiang University, Haining, China
chengting.21@intl.zju.edu.cn, ailiwang@intl.zju.edu.cn

Abstract

Spiking Neural Networks (SNNs), as one of the algorithmic models in neuromorphic computing, have gained a great deal of research attention owing to temporal information processing capability, low power consumption, and high biological plausibility. The potential to efficiently extract spatio-temporal features makes it suitable for processing the event streams. However, existing synaptic structures in SNNs are almost full-connections or spatial 2D convolution, neither of which can extract temporal dependencies adequately. In this work, we take inspiration from biological synapses and propose a spatio-temporal synaptic connection SNN (STSC-SNN) model, to enhance the spatio-temporal receptive fields of synaptic connections, thereby establishing temporal dependencies across layers. Concretely, we incorporate temporal convolution and attention mechanisms to implement synaptic filtering and gating functions. We show that endowing synaptic models with temporal dependencies can improve the performance of SNNs on classification tasks. In addition, we investigate the impact of performance via varied spatio-temporal receptive fields and reevaluate the temporal modules in SNNs. Our approach is tested on neuromorphic datasets, including DVS128 Gesture (gesture recognition), N-MNIST, CIFAR10-DVS (image classification), and SHD (speech digit recognition). The results show that the proposed model outperforms the state-of-the-art accuracy on nearly all datasets.

Introduction

Spiking neural networks (SNNs) are regarded as the third generation of neural networks (Maass 1997), with the purpose of addressing the fundamental mysteries of intelligence and the brain by emulating biological neurons and incorporating more biological mechanisms (Roy, Jaiswal, and Panda 2019). The two fundamental components of SNNs are spiking neurons and synapses, which create a hierarchical structure (layers) and subsequently construct a network. SNNs have attracted a significant deal of academic interest in recent years due to their prospective properties, such as the ability to process temporal information, low power consumption (Roy, Jaiswal, and Panda 2019), and biological interpretability (Gerstner et al. 2014). Currently, SNNs are capable of processing event stream data with low latency and low power (Pei et al. 2019; Gallego et al. 2020). However, there is still a performance gap between SNNs and traditional Artificial Neural Networks (ANNs). Recent SNN

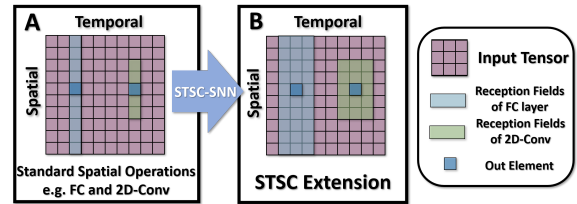


Figure 1: Illustration of Receptive Fields in Synaptic Connections. (a) The receptive fields of typical spatial operations used in SNNs, e.g., fully-connected layers (full) and 2D convolutional layers (sparse); (b) The STSC modules proposed to extend spatial operations with spatio-temporal receptive fields.

training techniques based on surrogate gradients and back-propagation have significantly enhanced the performance of SNNs (Wu et al. 2018; Fang et al. 2021b), while also promoting the further integration of ANNs’ modules into SNNs (Zheng et al. 2021; Hu, Tang, and Pan 2018; Yao et al. 2021), greatly accelerating the development of SNNs. However, it remains challenging to connect these computational techniques with the biological properties of SNNs.

Due to the time-dependent correlation of neuron dynamics, it is believed that SNNs naturally process information in both temporal and spatial dimensions (Roy, Jaiswal, and Panda 2019). Further researches are necessary to harness the spatio-temporal information processing capabilities of SNNs. Combining ANNs’ modules has significantly increased the performance of SNNs in several research studies. In terms of spatial information processing, CSNN (Xu et al. 2018) was the first to validate the application of convolution structure on SNNs, followed by the proposal of NeuNorm to improve SNNs’ usage of convolution through auxiliary neurons (Wu et al. 2019). In the time dimension, (Zheng et al. 2021) implements the time-dependent batch normalization (tdBN) module to tackle the issue of gradient vanishing and threshold balancing, and (Yao et al. 2021) uses the Squeeze-and-Excitation (SE) block (Hu, Shen, and Sun 2018) to realize the attention distribution of the temporal dimension in order to improve the temporal feature extraction. Notably, (Zhu et al. 2022) proposes Temporal-

Channel Joint Attention (TCJA) to concurrently process input in both temporal and spatial dimensions, which is a significant effort for SNNs' spatio-temporal feature extraction. These studies effectively improve the performance of SNNs by transplanting established ANNs' modules and methodologies. However, applying these computational modules to SNNs from the standpoint of deep learning dilutes the fundamental biological interpretability, bringing SNNs closer to a mix of existing concepts in machine learning, such as recurrent neural networks (RNNs), binary neural networks (BNNs), and quantization networks.

From a biological standpoint, some works focus on the synapse models, investigating the potential of SNNs in respect of connection modes and information transmission. (Shrestha and Orchard 2018; Fang et al. 2020a; Yu et al. 2022) integrate impulse response models with synaptic dynamics, hence enhancing the temporal information representation of SNNs; (Cheng et al. 2020) implements intra-layer lateral inhibitory connections to improve the noise tolerance of SNNs; from the standpoint of synaptic plasticity, (Bellec et al. 2020; Zhang and Li 2019) introduce bio-plausible training algorithms as an alternative to back-propagation (BP), allowing for lower-power training. Experiments revealed that the synaptic models of SNNs have a great deal of space for modification and refinement in order to handle spatio-temporal data better (Fang et al. 2020a). We propose a Spatio-Temporal Synaptic Connection (STSC) module for this reason.

Based on the notion of spatio-temporal receptive fields, the structural features of dendritic branches (Letellier et al. 2019) and feedforward lateral inhibition (Luo 2021) motivate this study. By merging the ANNs' computation modules (temporal convolutions and attention mechanisms) with SNNs, we propose the STSC module, consisting of Temporal Response Filter (TRF) module and Feedforward Lateral Inhibition (FLI) module. As shown in Fig. 1, the STSC can be attached to spatial operations to expand the spatio-temporal receptive fields of synaptic connections, hence facilitating the extraction of spatio-temporal features. The main contributions of this work are summarized as follows:

- We propose STSC-SNN to implement synaptic connections with extra temporal dependencies and enhance the SNNs' capacity to handle temporal information. To the best of our knowledge, this study is the first to propose the idea of synaptic connections with spatio-temporal receptive fields in SNNs and to investigate the influence of synaptic temporal dependencies in SNNs.
- Inspired by biological synapses, we propose two plug-and-play blocks: Temporal Response Filter (TRF) and Feedforward Lateral Inhibition (FLI), which perform temporal convolution and attention operations and can be simply implemented into deep learning frameworks for performance improvements.
- On neuromorphic datasets, DVS128 Gesture, SHD, N-MNIST, CIFAR10-DVS, we have produced positive results. Specifically, we acquire 92.36% accuracy on SHD with a simple fully-connected structure, which is a great improvement above the 91.08% results obtained with re-

current structure and reaches performance comparable to ANNs.

Related Work

Learning algorithms for SNNs

In recent years, many works have explored the learning algorithms of SNNs, which can be generally categorized as biologically inspired approaches (Diehl and Cook 2015; Bellec et al. 2020; Zhang and Li 2019), ANN-to-SNN conversion methods (Orchard et al. 2015; Sengupta et al. 2019; Han, Srinivasan, and Roy 2020), and surrogate-based direct training methods (Wu et al. 2018; Neftci, Mostafa, and Zenke 2019; Fang et al. 2021b). Direct training methods utilize surrogate gradients to tackle the issue of non-differentiable spike activity (Wu et al. 2018), allowing error back-propagation (BP) through time to interface the gradient descent directly on SNNs for training. Those BP-based methods show strong potential to achieve high accuracy in a few timesteps by making full use of spatio-temporal information (Wu et al. 2019; Fang et al. 2021b). However, more research is required to determine how to better extract spatio-temporal features for enhanced processing of spatio-temporal data; this is what we want to contribute.

Attention Modules in SNNs

The attention mechanism distributes attention preferentially to the most informative input components, which could be interpreted as the sensitivity of various inputs. The SE block (Hu, Shen, and Sun 2018) offers an efficient attention approach to improve representations in ANNs. (Xie et al. 2016; Kundu et al. 2021) introduced spatial-wise attention in SNNs; then, TA-SNN (Yao et al. 2021) developed a temporal-wise attention mechanism in SNNs by assigning attention factors to each input frame; more subsequently, TCJA (Zhu et al. 2022) added a channel-wise attention module and proposed temporal-channel joint attention. These studies demonstrate the usefulness of attention mechanisms in SNNs by achieving state-of-the-art results on various datasets. Moreover, based on these investigations, it is desirable to study other correlations between the attention mechanism and the biological nature of SNNs, which is the objective of our research. We employ the attention module as a feedforward lateral inhibitory connection (Luo 2021), which develops a gating mechanism for the synapse model, and enables nonlinear computation by the synapse.

Synaptic Models in SNNs

As one of the fundamental components of SNN, the synaptic model has drawn the interest of several researchers. (Shrestha and Orchard 2018; Fang et al. 2020a; Yu et al. 2022) established temporal relationships between response post-synaptic currents and input pre-synaptic spikes, therefore improving temporal expressiveness. Those temporal relationships are the extension of fully-connected synapses which are based on the assumption that there is only one connection between two neurons. Nevertheless, synaptic connections are often complex, and there are typically many paths connecting the axons and dendrites of neurons (Luo

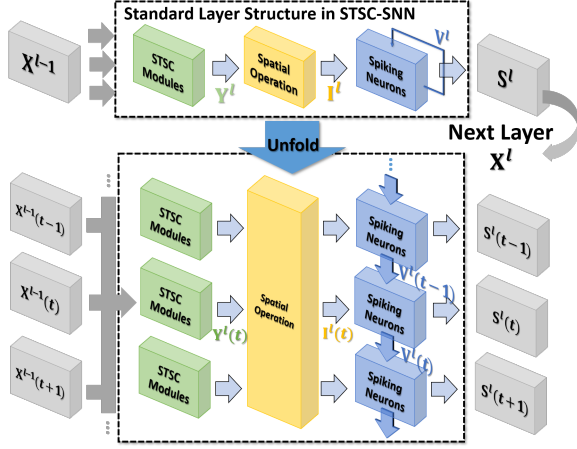


Figure 2: The standard layer inserted with the STSC module and its unfolded formulation. Note that all parameters are shared at all timesteps. STSC modules are set before spatial operations to process the latest temporal information.

2021; Letellier et al. 2019). We apply temporal convolution to describe the more sophisticated impulse response model and generate time-dependent post-synaptic currents, taking into consideration biological features and computational simplicity.

Approach

Frame-based Representation

Event stream consists of both a spatial and a temporal dimension, with the spatial dimension expandable to higher dimensions depending on the data type. The spatial dimension of event streams based on sound data is typically one-dimensional, corresponding to different frequency channels; whereas the spatial dimension of event streams based on image data is typically three-dimensional, consisting of coordinates representing spatial positions and polarities representing brightness changes. The binary spike pattern is represented by the tensor $E \in B^{T' \times S}$, where T' represents the original resolution in the temporal dimension, and S represents the resolution in the spatial dimension. For a frame with a time span of Δt , the events in the time interval $t' \in [(t-1) \times \Delta t, t \times \Delta t)$ can be mapped to the network input \mathbf{X}^0 at time t by

$$x^0(t) = q(\{E(t') | t' \in [(t-1) \times \Delta t, t \times \Delta t)\}) \quad (1)$$

where $t \in \{1, 2, \dots, T\}$ is timesteps, and the aggregation function $q(\cdot)$ could be chosen as non-polarity aggregation (Massa et al. 2020), accumulate aggregation (Deng et al. 2020), AND aggregation (He et al. 2020) etc. Here, we choose to accumulate all event streams inside a frame (see Fig. 4).

Spiking Neurons in SNNs

The Leaky-Integrate-and-Fire (LIF) model was introduced as an extremely simplified model of biological neurons

(Dayan and Abbott 2005), which has the essential qualities of potential integrating, leaking, and spike firing. The LIF model is used extensively in SNNs and neuromorphic engineering because of its ability to recreate essential neural functions at a minimal cost of computation. The LIF model is defined in the differential form, as

$$\tau \frac{dv(t)}{dt} = -v(t) + I(t) \quad (2)$$

where $v(t)$ is the membrane potential of the neuron at time t , $I(t)$ is the integrated current input from the pre-synaptic neuron at time t , and τ is the time constant that governs the pace of potential change. Solving the differential equation directly will incur additional costs. STBP (Wu et al. 2018) employs a simplified iterative representation and implements the LIF model on the Pytorch framework (Paszke et al. 2019), which supports the integration of SNNs and standard ANNs' modules and significantly speeds the construction of BP-based SNNs and training techniques. The explicit iterative LIF is expressed as

$$\mathbf{V}^l(t) = \left(1 - \frac{1}{\tau}\right) \times \mathbf{V}^l(t-1) \times (1 - \mathbf{S}^l(t-1)) + \mathbf{I}^l(t) \quad (3)$$

$$\mathbf{S}^l(t) = \Theta(\mathbf{V}^l(t) - V_{th}) \quad (4)$$

where l and t are indices of layer and time, τ is the time constant, \mathbf{V} is the membrane potential, V_{th} is the threshold constant, \mathbf{S} is the binary tensor of spikes, \mathbf{I} is the input from the preceding layer, and $\Theta(\cdot)$ is the Heaviside step function. Noting that the firing process, $\Theta(\cdot)$, is not differentiable, surrogate methods are often utilized in SNNs' direct training to achieve error propagation by creating various pseudo-derivatives for $\Theta(\cdot)$ (Neftci, Mostafa, and Zenke 2019). This work leverages arc tangent (ATan) as the pseudo-derivative of $\Theta(\cdot)$, which is well supported in the SpikingJelly framework (Fang et al. 2020b).

Spatio-Temporal Receptive Fields in SNNs

The receptive field is often used to comprehend convolution procedures. In the process of convolution, the receptive fields describe the range of the nearby input for identifying an output element, i.e., how much spatial neighboring position it can perceive. For static pictures, the receptive field could explain the projection range of the convolution operations and aid in the comprehension of the spatial feature extraction procedure. Similarly, the concept of receptive fields could be applied to event streams (or dynamic images) with an additional temporal dimension. This work leverages the concept of Spatio-Temporal Receptive Fields to aid comprehension of SNNs' spatio-temporal feature extraction procedure. As shown in Fig. 1a, typical synaptic connections employ 2D convolution, pooling, full-connections and other inter-layer computations to process information in the spatial dimension, which we refer to as spatial operations, and their receptive fields are restricted to the spatial dimension. To strengthen the spatio-temporal information processing capabilities of SNNs, it is essential to expand the receptive fields of these spatial operations into the temporal dimension.

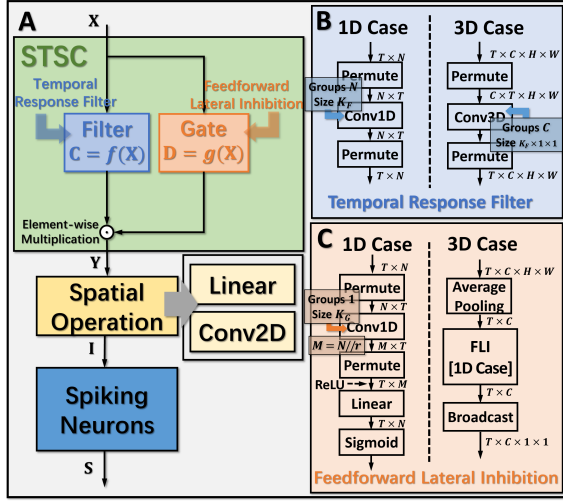


Figure 3: Operation Details of STSC modules. (a) Connection Implementation between TRF, FLI, and Spatial Operations, where \odot denotes broadcast element-wise multiplication; (b) Tensor Computations in TRF; (c) Tensor Computations in FLI.

Spatio-Temporal Synaptic Connection for SNNs

In general, the processing of temporal information in SNNs is attributed to spiking neurons, since their dynamic model has a natural dependence on the temporal dimension; however, the level of this dependence is primarily reliant on the degree of neural complexity, while the LIF neurons only support very weak temporal linkages. Not just in neurons, but also in biological synapses, a great deal of the processing of latent temporal characteristics occurs (Luo 2021; Letellier et al. 2019). This work focus on using temporal dimension operations in SNNs to broaden the spatio-temporal receptive fields of synapses, to enhance the spatio-temporal feature extractions of SNNs. Temporal operations are calculations connected to the time dimension, and they are contained in a pluggable module, referred to as the Spatio-Temporal Synaptic Connection (STSC). The STSC module is designed to be placed before spatial operations in order to aggregate temporal information and enlarge the spatio-temporal receptive fields while maintaining the original spatial operations (see Fig. 2). The STSC module consists of two modules: Temporal Response Filter and Feedforward Lateral Inhibition, which carry the filtering and gating mechanisms of the synaptic model, respectively (see Fig3). The two modules receive X as input tensor and conduct the operations $C = f(X)$ and $D = g(X)$, followed by element-wise product to produce output $Y = C \odot D$ (see Fig. 3a & Fig. 4).

Temporal Response Filter The synapses in biological neural networks are intricate. The complexity of synapses is not only reflected in the non-topological spatial relationship of synapses (how neurons connect with one another) but also in the complicated temporal dependency of spike transmission (how neurons communicate with one another) (Letellier

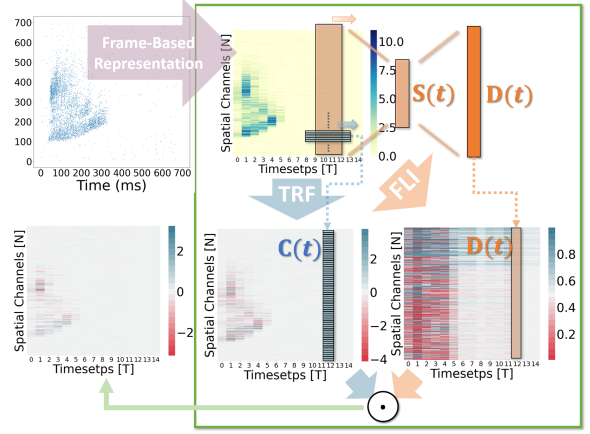


Figure 4: Computation Visualization. The input is an audio sample from the SHD dataset.

et al. 2019). This work proposes the Temporal Response Filter (TRF) to establish the linear response of spikes over time by employing convolution in the time dimension, in order to expand the temporal receptive field in the most direct way. TRF offers a filtering path for STSC with temporal convolutions (see Fig. 3). Fig. 3b depicts the specific implementation of TRF. In detail, as for the 2D spatiotemporal tensor in the fully-connected structure, it performs temporal depth-wise 1D convolution independently on each spatial channel and generates an output tensor of the same size. To ensure that all spatial elements inside a channel have the same temporal response, for the 4D spatiotemporal tensor in the convolutional structure, temporal depth-wise 3D convolution is performed on each channel with kernel size of $K_F \times 1 \times 1$. Mathematically, the filter operation is denoted as $f(\cdot)$, and it performs $C = f(X)$ with input X and output C having the same size as $R^{T \times N}$ or $R^{T \times C \times H \times W}$. Depending on the spatial dimension (1D or 3D) of the input X , the following calculation formulae apply:

As for the 1D case,

$$C(t, n) = \sum_{t_f = -\frac{K_F-1}{2}}^{\frac{K_F-1}{2}} \mathbf{W}_{t_f, n}^F \times \mathbf{X}(t - t_f, n) \quad (5)$$

As for the 3D case,

$$C(t, c, h, w) = \sum_{t_f = -\frac{K_F-1}{2}}^{\frac{K_F-1}{2}} \mathbf{W}_{t_f, c}^F \times \mathbf{X}(t - t_f, c, h, w) \quad (6)$$

where n, c, h , and w are spatial location indices and t is a time index. K_F denotes the kernel size of the temporal convolution, which is equal to the temporal receptive fields of TRF. The padding of the convolution is set to $\frac{K_F-1}{2}$ for maintaining the same size.

Feedforward Lateral Inhibition The mechanisms of feedforward lateral inhibition mechanisms exist in biological neural networks (Luo 2021), which construct a lateral

route to suppress feedforward input. We notice that the function of this structure closely resembles that of the attention module; therefore, we refer to the attention blocks (Hu, Shen, and Sun 2018; Yao et al. 2021; Zhu et al. 2022), and propose the FLI module to replicate the gating mechanism in synaptic connections. The module details are shown in Fig. 3c. Regarding the 2D spatiotemporal tensor in the fully-connected structure, temporal-wise 1D convolution is utilized first to extract temporal features, followed by linear combination through sigmoid to acquire the gating coefficients (see Fig. 3c). As for the 4D spatiotemporal tensor in the convolutional structure, spatial-wise average pooling is first conducted to obtain the channel-wise spatial sparsity of spikes; then, the 1D case FLI is performed. Finally, channel-wise gating factors are computed and transmitted to each channel’s spatial locations. Mathematically, gating is denoted as $g(\cdot)$, and \mathbf{X} is the input tensor of size $R^{T \times N}$ or $R^{T \times C \times H \times W}$, $\mathbf{D} = f(\mathbf{X})$ is the output gating factors with values in the range $(0, 1)$ that have the same shape with \mathbf{X} . Depending on the spatial dimension (1D or 3D) of the input \mathbf{X} , the following calculation equations apply:

As for the 1D case:

$$\mathbf{S}(t, m) = \sum_{t_g = -\frac{K_G-1}{2}}^{\frac{K_G-1}{2}} \sum_{n=1}^N \mathbf{W}_{t_g, n, m}^{G1} \times \mathbf{X}(t - t_g, n) \quad (7)$$

$$\mathbf{D}(t, n) = \text{Sigmoid} \left(\sum_{m=1}^M \mathbf{W}_{m, n}^{G2} \times \text{ReLU}(\mathbf{S}(t, m)) \right) \quad (8)$$

As for the 3D case:

$$\hat{\mathbf{X}}(t, c) = \frac{1}{H \times W} \sum_{h=1}^H \sum_{w=1}^W \mathbf{X}(t, c, h, w) \quad (9)$$

$$\hat{\mathbf{D}} = g_{1D}(\hat{\mathbf{X}}) \quad (10)$$

$$\mathbf{D}(t, c, h, w) = \hat{\mathbf{D}}(t, c) \quad \text{for } \forall h \in H, \forall w \in W \quad (11)$$

where n, c, h and w are spatial location indices, t is a time index, m is the index of the intermediate feature tensor S with spatial dimension M . M is determined by the spatial sizes N with reduction ratio r , as $\frac{N}{r}$. K_G denotes the kernel size of the convolution, which is equivalent to the receptive fields of FLI. The padding of the convolution is set to $\frac{K_G-1}{2}$ for maintaining the same size.

Training Framework

Denote the simulating timesteps as T , size of output layers as L_{out} and classes number as C , we utilize the voting strategy (Wu et al. 2019) to decode the network output $O \in B^{T \times L_{out}}$ with the constant voting matrix $M \in R^{C \times L_{out}}$. The loss function is defined by the mean squared error (MSE), as

$$L = \left\| \mathbf{y}_i - \frac{1}{T} \sum M_{i, n} O(t, n) \right\|^2 \quad (12)$$

where \mathbf{y} is the one-hot target, with $y_l = 1$ for target class l , and $y_i = 0$ for $i \neq l$. The predicted label l_p is then given

Datasets	SHD & CIFAR10-DVS & DVS128 Gesture & N-MNIST
Representation	Frames with Accumulative Aggregation
Learning Algorithm	STBP (Wu et al. 2018) & BPTT
Surrogate Gradient	ATan (Fang et al. 2021b)
Loss Function	Voting (Wu et al. 2019) & MSE
Frameworks	SpikingJelly & Pytorch

Table 1: Experimental Details.

Hyper Param.	SHD	N-MNIST	CIFAR10-DVS	DVS128 Gesture
Epoch	200	300	1000	1000
Batch Size	256	16	16	16
Learning Rate	1e-4	1e-3	1e-3	1e-3
T	15	10	10	20
τ	10	2	2	2
V_{th}	0.3	1.0	1.0	1.0
K_F	5	3	3	3
K_G	3	3	3	5
r	1	1	2	2

Table 2: Hyper-parameter Setting.

by $l_p = \text{argmax}_i \frac{1}{T} \sum M_{i, n} O(t, n)$ for evaluation. In the experiment, we adopted the simplest voting strategy and obtained $\sum M_{i, n} O(t, n)$ through average pooling.

Experiments

Experiment Setup

Datasets We evaluate the classification performance of STSC-SNN on a variety of neuromorphic datasets, including DVS128 Gesture (Amir et al. 2017) (gesture recognition), N-MNIST (Orchard et al. 2015) and CIFAR10-DVS (Li et al. 2017) (image classification), and SHD (Cramer et al. 2020) (speech digit recognition), all of which are event datasets but are generated using different methods. DVS128 Gesture is a gesture recognition dataset that uses DVS cameras to record actual human gestures. The event-based image datasets, N-MNIST and CIFAR10-DVS, are converted from the static dataset by using DVS cameras to scan each sample. Spiking Heidelberg Digits (SHD) is a spike-based speech dataset consisting of English and German spoken digits transformed from the audio recordings using an artificial inner ear model.

Learning Tab. 1 summarizes the experimental details of the SNNs training process. We use the SpikingJelly (Fang et al. 2020b) and Pytorch (Paszke et al. 2019) frameworks to develop and evaluate SNNs. We utilize the Adam optimizer (Kingma and Ba 2014) to accelerate the training process. Tab. 2 displays the respective hyper-parameters and Tab. 3 displays the network architectures for different datasets. All Conv2d layers are set as kernel size=3, stride=1, and padding=1, followed by batch normalization (BN) layers. The voting layers are implemented using average pooling for classification robustness (Fang et al. 2021b).

Dataset	Network Structure
DVS128 Gesture	Input-128C3-MP2-128C3-MP2-128C3-MP2-128C3-MP2-0.5DP-512FC-0.5DP-110FC-Voting-11
CIFAR10-DVS	Input-64C3-128C3-AP2-256C3-256C3-AP2-512C3-512C3-AP2-512C3-512C3-AP2-100FC-Voting-10
SHD	Input-128FC-128FC-100FC-Voting-20
N-MNIST	Input-128C3-AP2-128C3-AP2-0.5DP-2048FC-0.5DP-100FC-Voting-10

Table 3: Network Structure. The spiking neurons are added behind all xCy and nFC . The STSC modules are inserted before all xCy on DVS128 Gesture, CIFAR10-DVS, and N-MNIST; while inserted before all nFC on SHD.

Comparison with Existing SOTA Works

Tab. 4 shows the performance comparison of the proposed methods (STSC-SNN with TRF and FLI) and other competing methods on neuromorphic datasets, N-MNIST, CIFAR10-DVS, DVS128 Gesture, and SHD. As shown in Tab. 4, we achieve the highest accuracy on all datasets except CIFAR10-DVS. The SOTA results implemented in CIFAR10-DVS are based on the work of TET (Deng et al. 2022), which proposes a new loss function to enable the model to converge on a flatter local minimum with generalizability; TCJA (Zhu et al. 2022) also demonstrates its efficacy on CIFAR10-DVS. To preserve the consistency of this work, we continue to utilize MSE (Eq. (12)) as the loss function, and outperform the comparable result. Notably, the experiments on SHD show that we have enhanced the vanilla SNN from 78.71% to 92.36% using STSC, which is the state-of-the-art result compared to the highest available result (91.08% by TA-SNN). Moreover, it is a significant improvement that even reaches the best result achieved by ANNs on this dataset (92.4% by CNN (Cramer et al. 2020)). The SHD dataset contains rich temporal information, which challenges the model’s capacity to extract temporal features (Cramer et al. 2020); hence, there is considerable effort required to develop SNN models using recurrent structures (Cramer et al. 2020; Yin, Corradi, and Bohté 2020; Perez-Nieves et al. 2021; Yin, Corradi, and Bohté 2021). Based on the recurrent structure, TA-SNN employs temporal-wise attention and a particular LIF neuron (LIAF (Wu et al. 2021) that directly transmits membrane potential) to get an excellent result on SHD (91.08%), outperforming LSTM (89% (Cramer et al. 2020)) but falling short of the result (92.4%) produced by CNN processing (directly as 2D image input). In contrast, instead of the recurrent layers, we use a simple fully-connected network with two hidden layers and successfully obtain the SOTA result by adding the proposed STSC module. For the first time, our model obtained CNN-like performance on the SHD dataset, which represents a substantial effort to illustrate the SNNs’ potential.

Control Experiments and Ablation Study

To analyze the impact of each component on performance, we conduct control experiments on SHD. The SHD experiment is based on the fully-connected (FC) structure (see

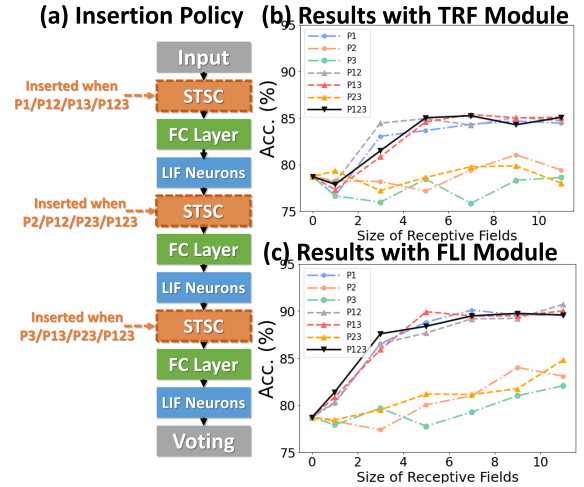


Figure 5: Control Experiments on SHD. (a) Policies of inserting STSC layers; (b) Accuracy comparison of TRF module via different RFs; (c) Accuracy comparison of FLI module via different RFs.

Tab. 3), with STSC modules strategically placed in front of the FC layers. There are seven insertion strategies designated P1, P2, P3, P12, P13, P23, and P123 (see Fig. 5a). Fig. 5b and 5c show the effect of varying receiving fields when TRF and FLI are used individually. TRF reaches 85.38% at P13 and RF=7, while FLI reaches 90.72% at P12 and RF=11. Comparing the two modules reveals that the FLI module plays a major role in performance improvement; thus, it is crucial to offer a gating mechanism that introduces nonlinear expressions to FC layers. Fig. 5b and 5c demonstrate that when the FLI or TRF modules are positioned in the first layer (P1/P12/P13/P123), they have a greater impact on performance than when they are positioned in the deep layer (P2/P3/P23). This suggests that the extraction of temporal features is more advantageous in shallow layers. As shown in Fig. 6, we evaluated the impact of varying STSC receptive fields on SHD performance. Notably, raising the receptive field suitably will increase performance, whereas an overly broad receptive field setting would reduce accuracy. We claim the performance drop is a result of the model’s excessive expressive capacity, which overfits the train data. This phenomenon is analogous to the usage of spatial 2D convolutions, in which the kernel size must be carefully determined. Fig. 6 indicates that the combination of TRF and FLI modules improves performance, demonstrating their complementarity. Under the P1 strategy, setting TRF’s RF=5 and FLI’s RF=3 yields the best result of 92.36%, with just one STSC added after the input layer.

Analysis of Temporal Modules in SNNs

In the vanilla SNNs, only neurons perform temporal operations; hence, its temporal feature extraction is predicated solely on the temporal dependence inside each neuron. In order to assess the influence of temporal modules, we con-

Method	SHD		N-MNIST		CIFAR10-DVS		DVS128 Gesture	
	T	Acc. (%)	T	Acc. (%)	T	Acc. (%)	T	Acc. (%)
NeuNorm (Wu et al. 2019)	-	-	-	99.53	-	60.5	-	-
Rollout (Kugele et al. 2020)	-	-	32	99.57	48	66.97	240	97.27 (10 classes)
LISNN (Cheng et al. 2020)	-	-	20	99.45	-	-	-	-
tdBN (Zheng et al. 2021)	-	-	-	-	10	67.8	40	96.87
LIAF-Net (Wu et al. 2021)	-	-	-	-	10	70.40	60	97.56
PLIF (Fang et al. 2021b)	-	-	10	99.61	20	74.80	20	97.57
LIF RSNN (Cramer et al. 2020)	2000	73.3	-	-	-	-	-	-
Hetero. RSNN (Perez-Nieves et al. 2021)	-	83.5	-	97.5	-	-	-	82.9
Adaptive SRNN (Yin, Corradi, and Bohté 2021)	250	90.4	-	-	-	-	-	-
SEW-ResNet (Fang et al. 2021a)	-	-	-	-	16	74.4	16	97.92
TA-SNN (Yao et al. 2021)	15	91.08	-	-	10	72.00	20	98.61
TET (Deng et al. 2022)	-	-	-	-	10	83.32	-	-
DSR (Meng et al. 2022)	-	-	-	-	10	77.41	-	-
TCJA (Zhu et al. 2022)	-	-	-	-	10	80.7(MSE)	20	99.0
STSC (this work)	15	92.4	10	99.64	10	81.4(MSE)	20	98.96

Table 4: Performance comparison between the proposed method and the state-of-the-art methods on different datasets.

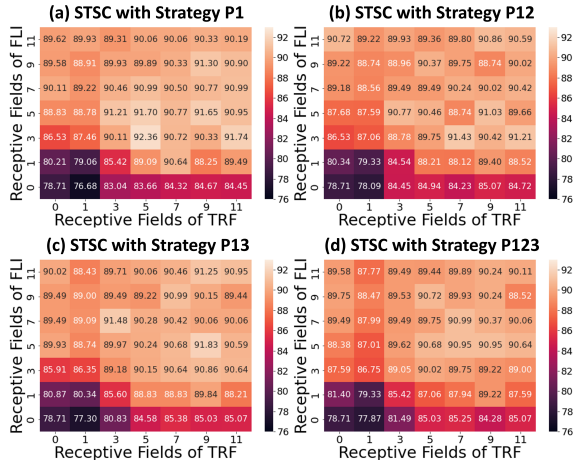


Figure 6: Influence of Receptive Fields on SHD. (a-d) show the experimental results via RFs with P1/P12/P13/P123.

duct the ablation study with LIF neurons and STSC modules on SHD datasets (see Fig. 7), based on the same FC structure (see Tab. 3). Experiments comparing 'FC(ReLU)' and 'SNN' demonstrate that utilizing LIF neurons to replace the activation function in the FC structure can definitely increase the performance of the SHD classification task, proving the LIF's capacity to handle temporal information and capture temporal features. Moreover, the 'FCs(ReLU)+STSC' and 'FCs(non)+STSC' structures generated by adding the STSC module obtain greater performance than the vanilla 'SNN' model, demonstrating that our STSC module has superior temporal feature extraction capacity than LIF; hence, the utilization of time relationships within synaptic connections is valid and meaningful. Furthermore, integrating the STSC module and LIF concurrently inside the 'SNN+STSC' model achieves the highest performance, proving that time-dependent interactions in both synapses and neurons could coexist and be coordinated to perform

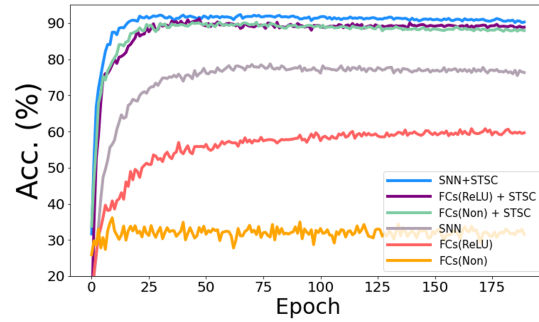


Figure 7: Ablation Study of Temporal Modules in SNNs. The accuracy comparison of different model via training epochs on SHD. 'FCs(Non)' denotes the FC structure without LIFs and activation functions, 'FCs(ReLU)' denotes the FC structure with ReLU functions behind the first two FC layers, and 'SNN' denotes the FC structure with LIFs behind all three FC layers. Then, STSC modules are added just behind input (P1) in three models as a comparison.

better temporal information processing.

Conclusion

This work proposes to endow synaptic structures with spatio-temporal receptive fields and additional temporal dependencies in an effort to enhance the temporal information processing capabilities of SNNs. We propose the STSC module from the standpoints of both computational models and biological realities, which consists of TRF and FLI, implemented with temporal convolution and attention mechanisms. We verified the method's reliability on neuromorphic datasets of SHD, N-MNIST, CIFAR10-DVS, and DVS Gesture. Notably, the STSC supports SNNs in reaching the SOTA result (92.36%) on the SHD dataset, which is comparable to ANNs' methods (89% and 92.4%), validating the potential of SNNs in the spatio-temporal data processing.

References

- Amir, A.; Taba, B.; Berg, D.; Melano, T.; McKinstry, J.; Di Nolfo, C.; Nayak, T.; Andreopoulos, A.; Garreau, G.; Mendoza, M.; et al. 2017. A low power, fully event-based gesture recognition system. In *Proceedings of the IEEE conference on computer vision and pattern recognition*, 7243–7252.
- Bellec, G.; Scherr, F.; Subramoney, A.; Hajek, E.; Salaj, D.; Legenstein, R.; and Maass, W. 2020. A solution to the learning dilemma for recurrent networks of spiking neurons. *Nature communications*, 11(1): 1–15.
- Cheng, X.; Hao, Y.; Xu, J.; and Xu, B. 2020. LISNN: Improving spiking neural networks with lateral interactions for robust object recognition. In *IJCAI*, 1519–1525.
- Cramer, B.; Stradmann, Y.; Schemmel, J.; and Zenke, F. 2020. The heidelberg spiking data sets for the systematic evaluation of spiking neural networks. *IEEE Transactions on Neural Networks and Learning Systems*.
- Dayan, P.; and Abbott, L. F. 2005. *Theoretical neuroscience: computational and mathematical modeling of neural systems*. MIT press.
- Deng, L.; Wu, Y.; Hu, X.; Liang, L.; Ding, Y.; Li, G.; Zhao, G.; Li, P.; and Xie, Y. 2020. Rethinking the performance comparison between SNNs and ANNs. *Neural networks*, 121: 294–307.
- Deng, S.; Li, Y.; Zhang, S.; and Gu, S. 2022. Temporal Efficient Training of Spiking Neural Network via Gradient Reweighting. *arXiv preprint arXiv:2202.11946*.
- Diehl, P. U.; and Cook, M. 2015. Unsupervised learning of digit recognition using spike-timing-dependent plasticity. *Frontiers in computational neuroscience*, 9: 99.
- Fang, H.; Shrestha, A.; Zhao, Z.; and Qiu, Q. 2020a. Exploiting neuron and synapse filter dynamics in spatial temporal learning of deep spiking neural network. *arXiv preprint arXiv:2003.02944*.
- Fang, W.; Chen, Y.; Ding, J.; Chen, D.; Yu, Z.; Zhou, H.; Tian, Y.; and other contributors. 2020b. SpikingJelly. <https://github.com/fangwei123456/spikingjelly>.
- Fang, W.; Yu, Z.; Chen, Y.; Huang, T.; Masquelier, T.; and Tian, Y. 2021a. Deep residual learning in spiking neural networks. *Advances in Neural Information Processing Systems*, 34: 21056–21069.
- Fang, W.; Yu, Z.; Chen, Y.; Masquelier, T.; Huang, T.; and Tian, Y. 2021b. Incorporating learnable membrane time constant to enhance learning of spiking neural networks. In *Proceedings of the IEEE/CVF International Conference on Computer Vision*, 2661–2671.
- Gallejo, G.; Delbrück, T.; Orchard, G.; Bartolozzi, C.; Taba, B.; Censi, A.; Leutenegger, S.; Davison, A. J.; Conrath, J.; Daniilidis, K.; et al. 2020. Event-based vision: A survey. *IEEE transactions on pattern analysis and machine intelligence*, 44(1): 154–180.
- Gerstner, W.; Kistler, W. M.; Naud, R.; and Paninski, L. 2014. *Neuronal dynamics: From single neurons to networks and models of cognition*. Cambridge University Press.
- Han, B.; Srinivasan, G.; and Roy, K. 2020. Rmp-snn: Residual membrane potential neuron for enabling deeper high-accuracy and low-latency spiking neural network. In *Proceedings of the IEEE/CVF conference on computer vision and pattern recognition*, 13558–13567.
- He, W.; Wu, Y.; Deng, L.; Li, G.; Wang, H.; Tian, Y.; Ding, W.; Wang, W.; and Xie, Y. 2020. Comparing SNNs and RNNs on neuromorphic vision datasets: Similarities and differences. *Neural Networks*, 132: 108–120.
- Hu, J.; Shen, L.; and Sun, G. 2018. Squeeze-and-excitation networks. In *Proceedings of the IEEE conference on computer vision and pattern recognition*, 7132–7141.
- Hu, Y.; Tang, H.; and Pan, G. 2018. Spiking Deep Residual Networks. *IEEE Transactions on Neural Networks and Learning Systems*.
- Kingma, D. P.; and Ba, J. 2014. Adam: A method for stochastic optimization. *arXiv preprint arXiv:1412.6980*.
- Kugele, A.; Pfeil, T.; Pfeiffer, M.; and Chicca, E. 2020. Efficient processing of spatio-temporal data streams with spiking neural networks. *Frontiers in Neuroscience*, 14: 439.
- Kundu, S.; Datta, G.; Pedram, M.; and Bearel, P. A. 2021. Spike-thrift: Towards energy-efficient deep spiking neural networks by limiting spiking activity via attention-guided compression. In *Proceedings of the IEEE/CVF Winter Conference on Applications of Computer Vision*, 3953–3962.
- Letellier, M.; Levet, F.; Thoumine, O.; and Goda, Y. 2019. Differential role of pre-and postsynaptic neurons in the activity-dependent control of synaptic strengths across dendrites. *PLoS biology*, 17(6): e2006223.
- Li, H.; Liu, H.; Ji, X.; Li, G.; and Shi, L. 2017. Cifar10-dvs: an event-stream dataset for object classification. *Frontiers in neuroscience*, 11: 309.
- Luo, L. 2021. Architectures of neuronal circuits. *Science*, 373(6559): eabg7285.
- Maass, W. 1997. Networks of spiking neurons: the third generation of neural network models. *Neural networks*, 10(9): 1659–1671.
- Massa, R.; Marchisio, A.; Martina, M.; and Shafique, M. 2020. An efficient spiking neural network for recognizing gestures with a dvs camera on the loihi neuromorphic processor. In *2020 International Joint Conference on Neural Networks (IJCNN)*, 1–9. IEEE.
- Meng, Q.; Xiao, M.; Yan, S.; Wang, Y.; Lin, Z.; and Luo, Z.-Q. 2022. Training High-Performance Low-Latency Spiking Neural Networks by Differentiation on Spike Representation. In *Proceedings of the IEEE/CVF Conference on Computer Vision and Pattern Recognition*, 12444–12453.
- Neftci, E. O.; Mostafa, H.; and Zenke, F. 2019. Surrogate gradient learning in spiking neural networks: Bringing the power of gradient-based optimization to spiking neural networks. *IEEE Signal Processing Magazine*, 36(6): 51–63.
- Orchard, G.; Jayawant, A.; Cohen, G. K.; and Thakor, N. 2015. Converting static image datasets to spiking neuromorphic datasets using saccades. *Frontiers in neuroscience*, 9: 437.

- Paszke, A.; Gross, S.; Massa, F.; Lerer, A.; Bradbury, J.; Chanan, G.; Killeen, T.; Lin, Z.; Gimelshein, N.; Antiga, L.; et al. 2019. Pytorch: An imperative style, high-performance deep learning library. *Advances in neural information processing systems*, 32.
- Pei, J.; Deng, L.; Song, S.; Zhao, M.; Zhang, Y.; Wu, S.; Wang, G.; Zou, Z.; Wu, Z.; He, W.; et al. 2019. Towards artificial general intelligence with hybrid Tianjic chip architecture. *Nature*, 572(7767): 106–111.
- Perez-Nieves, N.; Leung, V. C.; Dragotti, P. L.; and Goodman, D. F. 2021. Neural heterogeneity promotes robust learning. *Nature communications*, 12(1): 1–9.
- Roy, K.; Jaiswal, A.; and Panda, P. 2019. Towards spike-based machine intelligence with neuromorphic computing. *Nature*, 575(7784): 607–617.
- Sengupta, A.; Ye, Y.; Wang, R.; Liu, C.; and Roy, K. 2019. Going deeper in spiking neural networks: VGG and residual architectures. *Frontiers in neuroscience*, 13: 95.
- Shrestha, S. B.; and Orchard, G. 2018. Slayer: Spike layer error reassignment in time. *Advances in neural information processing systems*, 31.
- Wu, Y.; Deng, L.; Li, G.; Zhu, J.; and Shi, L. 2018. Spatio-temporal backpropagation for training high-performance spiking neural networks. *Frontiers in neuroscience*, 12: 331.
- Wu, Y.; Deng, L.; Li, G.; Zhu, J.; Xie, Y.; and Shi, L. 2019. Direct training for spiking neural networks: Faster, larger, better. In *Proceedings of the AAAI Conference on Artificial Intelligence*, volume 33, 1311–1318.
- Wu, Z.; Zhang, H.; Lin, Y.; Li, G.; Wang, M.; and Tang, Y. 2021. Liaf-net: Leaky integrate and analog fire network for lightweight and efficient spatiotemporal information processing. *IEEE Transactions on Neural Networks and Learning Systems*.
- Xie, X.; Qu, H.; Yi, Z.; and Kurths, J. 2016. Efficient training of supervised spiking neural network via accurate synaptic-efficiency adjustment method. *IEEE transactions on neural networks and learning systems*, 28(6): 1411–1424.
- Xu, Q.; Qi, Y.; Yu, H.; Shen, J.; Tang, H.; Pan, G.; et al. 2018. Csn: an augmented spiking based framework with perceptron-inception. In *IJCAI*, 1646–1652.
- Yao, M.; Gao, H.; Zhao, G.; Wang, D.; Lin, Y.; Yang, Z.; and Li, G. 2021. Temporal-wise attention spiking neural networks for event streams classification. In *Proceedings of the IEEE/CVF International Conference on Computer Vision*, 10221–10230.
- Yin, B.; Corradi, F.; and Bohté, S. M. 2020. Effective and efficient computation with multiple-timescale spiking recurrent neural networks. In *International Conference on Neuromorphic Systems 2020*, 1–8.
- Yin, B.; Corradi, F.; and Bohté, S. M. 2021. Accurate and efficient time-domain classification with adaptive spiking recurrent neural networks. *Nature Machine Intelligence*, 3(10): 905–913.
- Yu, C.; Du, Y.; Chen, M.; Wang, A.; Wang, G.; and Li, E. 2022. MAP-SNN: Mapping Spike Activities with Multiplicity, Adaptability, and Plasticity into Bio-Plausible Spiking Neural Networks. *arXiv preprint arXiv:2204.09893*.
- Zhang, W.; and Li, P. 2019. Spike-train level backpropagation for training deep recurrent spiking neural networks. *Advances in neural information processing systems*, 32.
- Zheng, H.; Wu, Y.; Deng, L.; Hu, Y.; and Li, G. 2021. Going deeper with directly-trained larger spiking neural networks. In *Proceedings of the AAAI Conference on Artificial Intelligence*, volume 35, 11062–11070.
- Zhu, R.-J.; Zhao, Q.; Zhang, T.; Deng, H.; Duan, Y.; Zhang, M.; and Deng, L.-J. 2022. TCJA-SNN: Temporal-Channel Joint Attention for Spiking Neural Networks. *arXiv preprint arXiv:2206.10177*.